JOURNAL OF AGRICULTURAL AND FOOD CHEMISTRY

pubs.acs.org/JAFC Article

Ice Recrystallization Inhibition Activity of Soy Protein Hydrolysates

Madison Fomich, Vermont P. Día, Uvinduni I. Premadasa, Benjamin Doughty, Hari B. Krishnan, and Tong Wang*

Cite This: https://doi.org/10.1021/acs.jafc.2c08701 Read Online

ACCESS | Metrics & More | Article Recommendations

ABSTRACT: Identifying and developing ice recrystallization inhibitors from sustainable food proteins such as soy protein isolate (SPI) can lead to practical applications in both pharmaceutical and food industries. The objective of this study was to investigate the ice recrystallization inhibition (IRI) activity of SPI hydrolysates, and this was achieved by using an IRI activity-guided fractionation approach and relating IRI activity to interfacial molecular activity measured by vibrational sum frequency generation (VSFG). In addition, the impact of molecular weight (MW) and enzyme specificity was analyzed using three different proteases (Alcalase, trypsin, and pancreatin) and varying hydrolysis times. Using preparative chromatography, hydrolysates from each enzyme treatment were fractionated into five different MW fractions (F1−F5), which were then characterized by high-performance liquid chromatography (HPLC). All SPI hydrolysates had IRI activity, resulting in a 57−29% ice crystal diameter reduction when compared to native SPI. The F1 fraction (of 4−14 kDa) was most effective among all tested hydrolysates, while the lower MW peptide fractions lacked activity. One sample (SPI-ALC 20-F1) had a 52% reduction of ice crystal size at a lower concentration of 2% compared to the typical 4% used. SFG showed a difference in H-bonding and hydrophobic interactions of the molecules on the water/air interface, which may be linked to IRI activity. This study demonstrates for the first time the ability of SPI hydrolysates to inhibit ice crystal growth and the potential application of SFG to study molecular interaction at the interface that may help illustrate the mechanism of action.

KEYWORDS: *soy protein, antifreeze peptides, ice recrystallization inhibition, enzymatic hydrolysis*

INTRODUCTION

Ice recrystallization is a form of Ostwald's ripening that is a process when larger ice crystals expand at the expense of smaller crystals within a frozen matrix.[1,2] This change can deteriorate the quality of frozen foods over time, resulting in eventual freezer burn and the loss of textural properties in some foods.[3] Ice recrystallization at sub-freezing temperatures also creates harsh living environments for many organisms. Organisms that survive in sub-zero climates such as insects, polar fish, bacteria, and arctic plants produce antifreeze proteins (AFPs) to prevent ice crystallization that can harm them.[1,4−14] Ice recrystallization inhibition (IRI) is the result of the interaction of an IRI active agent, the ice crystal, and the surrounding water that prevents the expansion of the ice crystals. To date, multiple hypotheses of IRI have been proposed,[1,15] but there is no one universal mechanism. Uncovering important characteristics of IRI active agents and deriving the mechanisms of IRI activity for a specific group of compounds could lead to the development of new IRI agents, which can then be used to limit ice crystal growth in frozen foods and prevent damage to food's microstructure.

There are different types of AFPs found in nature that possess a variety of structures, molecular weights (MWs), amino acid sequences, and amphiphilicity.[4] Among the wide variety in structural characteristics, it is thought that the AFPs must be amphiphilic to partition to ice or ice−water interface to inhibit the addition of water to the ice surface.[1,5,16,17] This is accomplished by having polar hydrophilic groups that can contribute to hydrogen bonding with the ice crystal's lattice as an anchor and hydrophobic groups to prevent other water molecules from adsorbing to the surface to form a new layer of ice.[13,16−18] Since the role of hydrogen bonding and hydrophobic interactions at the water and ice interface is hypothesized to be important for IRI activity, being able to characterize changes in hydrogen bonding and molecular assembly at aqueous interfaces may serve as an indication of IRI activity.

The use of natural AFPs in the food industry would help reduce the quality deterioration from ice recrystallization and increase the shelf life of frozen foods.[19,20] However, the extraction and purification of natural AFPs are not economically feasible, and these proteins are limited in nature. If protein-derived molecules can be produced that possess important characteristics observed in natural AFPs to inhibit ice crystal growth, then these molecules could be a feasible solution for use in the food industry.

While proteins are nature's approach to IRI, other molecules have been studied in this context including hydrocolloids,

Received: December 9, 2022
Revised: June 14, 2023
Accepted: June 15, 2023

polysaccharides, and protein hydrolysates. Various animal source proteins, such as fish skin,[18] tilapia scales,[21] pig skin,[22−25] chicken skin,[26] bovine gelatin,[27,28] and shark skin,[29,30] have been used to produce IRI active peptides. All these sources produced IRI active peptides in the size range of 880−6000 Da by protease hydrolysis.[22−30] Even though gelatin hydrolysates have been shown to have IRI activity, other proteins and peptides may have the potential to exhibit IRI activity, since AFPs have a variety of sizes, secondary structures, and amino acid compositions and sequences that can contribute to IRI activity.[1] All of the peptide sources discussed above are animal-based, so the utilization of an alternative plant protein, such as soy protein isolate (SPI), would present a more abundant option that would be allowed in a variety of frozen products including vegan and vegetarian options.

SPI has recently been shown to possess IRI activity after Alcalase hydrolysis for 15 and 60 min,[31] significantly reducing the MLGS by 52%.[31] However, this report is focused on how enzyme specificity, MW, and other molecular characteristics impact the IRI activity of SPI hydrolysates. This study is necessary to optimize IRI activity and understand how peptide molecular features relate to the activity.[31]

To better understand the IRI activity of SPI peptides of different molecular characteristics, a set of hydrolysates were made using different enzymes to produce samples with differing MW distributions. Then, peptide size and other characteristics were investigated to understand the differences among the hydrolysates and explore the key factors contributing to the IRI activity of SPI hydrolysates. Hence, the objectives of this work were to generate IRI active peptides from SPI with varying MWs, characterize the samples to understand how different enzyme specificities and MWs influence the IRI activity of the peptides, analyze how the peptides influence the ordering and hydrogen bonding of water at the interface, and rationalize how this relates to IRI activity.

MATERIALS AND METHODS

Materials. SPI was obtained from Bulksupplements.com (Henderson, NV). The enzyme Alcalase was purchased from Millipore Corp (Billerica MA, Product # 126741), pancreatin from Sigma-Aldrich (St. Louis, MO, CAS # 8049-47-6), and trypsin from Thermo Fisher Scientific (Ward Hill, MA, CAS # 9002-07-7). *o*-Phthaldialdehyde (OPA) was obtained from MP Biomedical (Solon, OH, CAS # 643-79-8), SDS-PAGE-buffer and Coomassie blue stain were obtained from Bio-Rad Laboratories (Hercules, CA). SDS-PAGE gels and the protein MW standard were obtained from Genscript Biotech (Piscataway, NJ). The HPLC standard was created with analytical grade albumin, aprotinin, glucagon, bradykinin acetate, bradykinin 1−5, glutathione, and glycine, which were all purchased from Sigma-Aldrich (St. Louis, MO). The reagents and chemicals, acetonitrile, methanol, trifluoroacetic acid (TFA), ammonium bicarbonate, and PBS, were obtained from Thermo Fischer Scientific (Ward Hill, MA). The positive control poly(vinyl alcohol) (PVA) was obtained from Sigma-Aldrich (St. Louis, MO, CAS # 9002-89-5, MW 89,000-98,000 Da), and the negative control poly(ethylene glycol) (PEG) was from Tokyo Chemical Industry (Tokyo, Japan, CAS # 25322-68-3, MW 400 Da).

Enzymatic Hydrolysis to Create SPI Peptides of Various MWs. All enzymatic hydrolyses were performed at their respective optimum conditions (Alcalase (ALC) at 55 °C, pH 8; pancreatin (PAN) at 40 °C, pH 8; and trypsin (TRY) at 37 °C, pH 8.0−9.0). A 10% SPI dispersion was placed in a 250 mL bottle, and the pH was adjusted to the optimum level. This bottle was then placed in a water bath at an appropriate temperature and allowed to equilibrate. The enzyme was added at specific concentrations based on enzyme type (ALC at 0.176 Au/g, PAN at 3.23 Au/g, TRY at 280 Au/g), and sample aliquots were taken at various times depending on the enzyme used (for ALC, at 2, 5, 10, 20, 30, 40 min; for PAN, at 5, 15, 30, 60, 120, 240 min; and for TRY, at 30, 60, 90, 120, 240, 1440 min). The samples were placed in a boiling water bath for 10 min to inactivate the enzyme and centrifuged at 15 000*g* for 10 min at 4 °C. The supernatant of each sample was collected, freeze-dried, and used for further analysis.

Fractionation of Soy Hydrolysates Using Size Exclusion Chromatography. Certain treatments or samples were fractionated using preparative medium pressure size exclusion chromatography. Samples with different concentrations (75−120 mg/mL) were dissolved in 100 mM ammonium bicarbonate buffer, centrifuged, and then filtered through a 0.22 μm syringe filter before fractionation. Separation was performed using the AKTA protein purification system (General Electric, Boston, MA) equipped with a UV detector (280 nm). Each sample consisting of 5 mL of a 75−120 mg/mL solution was injected into a Hiload 16/600 30 pg (MW range of 1−10 kDa, General Electric, Boston, MA) column and eluted at 1 mL/min for 160 min. Samples were collected by an F9-R collector (General Electric, Boston, MA) and separated into five fractions according to UV detection, generating different volumes for each fraction as discussed later. The ammonium bicarbonate was removed from the solution via decomposition at 85 °C for 6 h. Then, the samples were freeze-dried for further analysis.

HPLC Method to Determine the Peptide Size of SPI Hydrolysates and Fractions. The MW distribution for each of the hydrolysate and fractionated samples was analyzed using a size exclusion (Phenomenex BioSep-SEC -s2000 column) HPLC. Samples of 20 μL of 1 mg/mL concentration were injected and eluted for 20 min using a 45% acetonitrile and 0.1% TFA solution and detected using a UV detector at 214 nm. To determine the average molecular size and distribution of each of the samples, the elution profile was compared to a standard to determine the range of molecular size. The standards used were albumin (1 mg/mL, MW = 66 000 Da), glycine (6 mg/mL, MW = 75 Da), and a mixed standard containing aprotinin (MW = 6500 Da), glucagon (MW = 3842 Da), bradykinin acetate (MW = 1060 Da), bradykinin 1−5 (MW = 573 Da), and glutathione (MW = 307 MW; all at 1−1.5 mg/mL). Average MW was calculated using the log−linear relationship between retention time and MW to create a standard curve. The area for each retention time interval was then used to calculate which proportion of the peptide sample was in that size range. All peaks were added together to obtain a weighted average MW for each sample.

OPA Method to Determine the Relative Degree of Hydrolysis. The degree of hydrolysis (DOH) of the peptide samples was determined based on a previous procedure with slight modifications.[32] The OPA reagent was prepared in a mixture of 25 mL of 100 mM borax, 2.5 mL of a 20% SDS solution, a solution of 40 mg of OPA dissolved in 1 mL of methanol, 100 μL of β-mercaptoethanol, and DI water adjusting the solution to a total volume of 50 mL. A peptide sample of 10 μL (1 mg/mL in 1× PBS buffer) was placed in a 96-well plate and 200 μL of freshly prepared OPA reagent was added. Four blank wells were also filled with 10 μL 1× PBS buffer (2 wells) and 10 μL of 1 mg/mL fully hydrolyzed SPI (2 wells). The absorbance was read immediately at 340 nm using a Cambrex ELx808 microplate reader. DOH was calculated using the following formula

$$\mathrm{DOH} = \frac{\text{absorbance of 1 mg/mL hydrolysate}}{\text{absorbance of 1 mg/mL fully hydrolyzed SPI}} \times 100$$

Splat Assay to Analyze IRI Activity of Fractions and Hydrolysates. A standard procedure was used to quantify the IRI activity of the hydrolysates and fractions. The assay[33] was performed with 4% w/w solutions of the hydrolysates dissolved in 1× PBS buffer. One drop was delivered from 1.5 m height onto a precooled microscope slide at −80 °C. The slide was then annealed at −8 °C using a cryo-stage HCS 302 (Instec Instruments, Boulder, CO) for 30 min, with pictures taken using a polarized light microscope (Leica, DM2700 M, Wetzlar, Germany) with a built-in digital camera (Leica,

https://doi.org/10.1021/acs.jafc.2c08701
J. Agric. Food Chem. XXXX, XXX, XXX−XXX

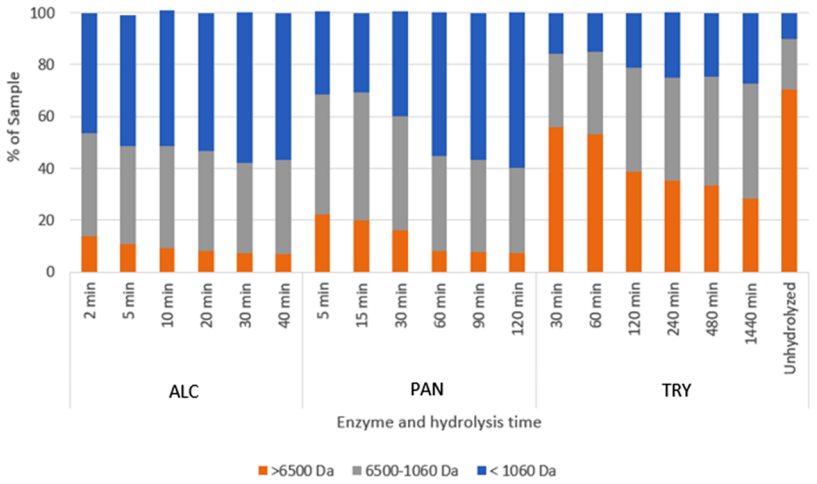

Figure 1. MW distribution as a % of each MW fraction relative to the total in the samples prepared by ALC, PAN, and TRY hydrolysis for various lengths of times as measured by HPLC.

DMC 4500, Wetzlar, Germany). Mean large grain size (MLGS) was obtained by measuring the diameter of the 10 largest ice crystals in each image. An average from 2 repeated hydrolyses with 2 drops from each sample and 3 images for each drop resulted in a total of 12 images per sample.

MW Profile of Hydrolysates by Sodium Dodecyl Sulfate-Polyacrylamide Gel Electrophoresis (SDS-PAGE). The profiles of peptide components in the SPI hydrolysates and fractions were analyzed by SDS-PAGE under a reducing condition using an 8−16% SurePAGE, Bis-Tris 10 × 8 gel (GenScript Biotech, Piscataway, NJ). The samples were mixed at a 95:5 ratio with β-mercaptoethanol. Each well was filled with 10 μL of 1:1 sample and 2× Laemmli sample buffer (Bio-Rad Laboratories, Hercules, CA), resulting in a total of 25 μg of hydrolysate in each well. Electrophoresis was performed on a BIO-RAD PowerPac Basic (Bio-Rad Laboratories, Hercules, CA) at 400 mA and 140 V for 70 min. The running buffer used was 1 L of 1× Tris/glycine/SDS buffer with the final concentration of 25 mM Tris, 192 mM glycine, and 0.1% w/v SDS at a pH of 8.3. After electrophoresis, peptide bands were fixed with a solution containing 40% methanol and 10% acetic acid before staining with Bio-Safe Coomassie G-250 Stain (Bio-Rad Laboratories, Hercules, CA) for 2 h. After staining, the gel was washed with DI water overnight with water being changed as needed to remove excess dye.

Vibrational Sum Frequency Generation to Probe Peptide-Decorated Air/Aqueous Interfaces. Vibrational sum frequency generation (SFG) spectroscopy measurements were performed on selected samples (SPI-ALC-20, SPI-PAN-60, SPI-TRY-120, abbreviations shown are SPI-enzyme used-time of hydrolysis in minutes), all their respective F1 fractions, unhydrolyzed SPI, PEG (negative control), and PVA (positive control) using a previously described instrument.[34−36] Briefly, the output of a femtosecond laser system was split to produce mid-infrared (IR) light centered near 2900 or 3300 cm^{-1}, depending on the vibrational modes of interest. Time-symmetric narrowband near-infrared (NIR) pulses (~1 ps centered at ~803 nm) were generated in a second path equipped with a pulse shaping device and used for upconversion. Light from both paths was spatially and temporally overlapped at the sample interface in a colinear excitation geometry. The radiated SFG light was collected with an achromatic doublet, polarization-resolved, and dispersed in a spectrograph (Andor Kymera 328*i*) for detection with an electron-multiplying CCD camera (Andor Newton). SFG spectra were acquired in the SSP polarization combination at the air/sample interface (the letters describing the polarization combinations refer to the sum of SFG, NIR, and IR light fields, respectively). The spectral profile was corrected using a reference spectrum collected from a gold film in the PPP polarization combination. Background spectra were collected frame-for-frame using a co-specified region of interest.

LC-MS Analysis of Active Hydrolysate Fractions for Molecular Species Profile Analysis. *Sample Preparation.* An aliquot was weighed out (between 0.5 and 2 mg) and resuspended at 5 mg/mL in a 5% acetonitrile/0.1% formic acid solvent. Samples were vortexed at room temperature for 5 min and centrifuged at 16 000*g*, and then the supernatants were transferred to vials and placed in a cooled autosampler (7 °C).

Mass Spectrometry. Peptides were analyzed by mass spectrometry as follows: a 5 μL injection was made onto a C18 trap column (Thermo Scientific, u-Precolumn, C18 PepMap100, 5 mm × 300 μm, 5 μm particles) for in-line desalting, and the peptides were separated using an 11 cm long × 150 μm inner diameter pulled-needle analytical column packed with HxSIL-C18, 5 μm reversed phase resin (The Hamilton Co., Reno, NV). Peptides were eluted from the analytical column with gradient elution using acetonitrile at 400 nL/min. The Proxeon/Thermo Easy nLC was integrated with a Thermo LTQ Orbitrap using Xcalibur V2.0.LC gradient elution: initial conditions were 2%B (A: 0.1% formic acid in water, B: 99.9% acetonitrile, 0.1% formic acid), followed by 2 min ramp to 20% B, 20−30% B over next 15 min, 30−90% B over 5 min, holding at 90% B for 13 min, and finally, ramping back to (1 min) and holding (4 min) initial conditions. The total run time was 45 min. MS data were collected in positive-ion FTMS (Orbitrap) mode at 1.6 kV using the following parameters: 30 000 resolution, 1 microscan, 300−1800 m/z, profile, and then for each cycle (lasting ~3 s), the most abundant peptides (ignored trypsin autolysis ions and all + 1 ions, >1000 counts) were selected for ion-trap CID MSMS (2 m/z mass window, 35% normalized collision energy, centroid). Dynamic exclusion was enabled with the following parameters: repeat count 1, repeat duration 30 s, exclusion list 500, exclusion duration 180 s.

Statistical Analysis. Ice crystal measurement data for each hydrolysate and fraction were made in duplicates. The mean largest grain size (MLGS) is reported as an average of duplicate hydrolysates. Tukey's test was performed using JMP to compare means, and the significance level at $p = 0.05$ was used.

RESULTS AND DISCUSSION

Studies of antifreezing proteins have demonstrated strong ice-binding characteristics of these naturally occurring proteins. However, not all antifreezing agents are ice-binding. There are many natural and synthetic small or large molecules that are strong IRI agents, but they do not bind to the ice surface, and their modes of action are different and the mechanisms are not all fully understood.[37] Protein hydrolysates have been reported as IRI agents; however, no report has been seen to illustrate the mechanism of action, possibly due to the difficulty in

https://doi.org/10.1021/acs.jafc.2c08701
J. Agric. Food Chem. XXXX, XXX, XXX−XXX

studying such complex molecular mixtures. This work is the first report of our work with the aim of producing and characterizing IRI active peptide mixtures and proposing and testing the hypothesis of their IRI activity.

Effect of the Extent of SPI Hydrolysis and the Type of Enzyme on IRI Activity. The MW of the protein hydrolysate is directly related to the extent of enzymatic hydrolysis and the specificity of the proteases. ALC, TRY, and PAN are different proteases with molecular weights of 27 000, 23 300, and 25 700 Da, respectively,[38−41] and they have different specificities on the cleavage of the peptide bonds of the proteins. ALC is a random protease and will cleave the protein at random points in the peptide chain;[38] TRY is amino acid specific and will only hydrolyze sites next to lysine and arginine;[41] PAN is a complex mixture of enzymes but has two predominant amino acid specific enzymes, TRY and chymotrypsin.[40] Chymotrypsin is also a specific protease that cleaves bonds next to tryptophan, tyrosine, and phenylalanine.[42] This would result in a greater DOH than TRY, but it will also lack the randomness of ALC hydrolysis. Due to the difference in enzymatic specificity, the peptide chain length and properties of the peptides can be different based on the protease used and the extent of hydrolysis. Figure 1 shows the MW distribution of the SPI hydrolysates after ALC, TRY, and PAN hydrolysis at various times. As expected, the percentage of peptides smaller than 1 kDa increased as hydrolysis time was increased for all enzymes. Similarly, the samples hydrolyzed by the random protease (ALC) contained the largest quantity of smaller peptides over a shorter time of hydrolysis. The average MW of the peptides decreased as hydrolysis time was increased as reflected by the DOH and average MW, as summarized in Table 1. By using enzymes with differing specificity and varying hydrolysis times, hydrolysates with a range of average MWs and DOH were produced, which allowed the determination of the impact of the type of enzyme specificity and the extent of hydrolysis on IRI activity.

For the determination of IRI activity, both qualitative and quantitative aspects were measured using the splat assay. Images taken under a microscope at −8 °C for 30 min were used to generate the MLGS, and the data are summarized in Table 1 and Figure 2, which shows representative images. Notably, at a 4% hydrolysate concentration, every SPI hydrolysate had IRI activity, as shown in Table 1. In addition, enzyme specificity did play a significant role in IRI activity. The peptides produced from PAN hydrolysis had lower activity when compared to ALC and TRY hydrolysates. Since PAN is a mixture of TRY and chymotrypsin, the chymotrypsin hydrolysis may be responsible for the decrease in IRI activity compared to the hydrolysates with only TRY that demonstrated strong IRI activity. This could be due to the specificity of the chymotrypsin to cut at hydrophobic aromatic amino acid residues, which would expose these residues on the end of the peptide chains.

It is worth noting that the proteases themselves were tested at the concentrations used for hydrolysis in a negative PEG sample and they did not show IRI activity, as shown in Table 1. All MLGS values were not statistically different from the initial PEG negative control or had lower activity. Each peptide sample also contained the same concentration of the corresponding enzyme, and a reduction in IRI activity was observed after SPI hydrolysis. Therefore, we speculate that there was no enzyme-induced activity, and the IRI activity is attributed to the peptides generated by hydrolysis.

Table 1. Mean Largest Grain Size (MLGS) of Ice Crystals for Samples Tested at 4% Concentration, Average MW, and DOH of the Whole SPI Hydrolysates Made by ALC, PAN, and TRY

enzyme	hydrolysis time (min)	average MW (Da)	DOH	MLGS (μm)
ALC	2	3409	17.4	26.6 ± 3.1^{a}
	5	2747	19.9	27.1 ± 1.9^{a}
	10	2727	21.5	25.9 ± 4.5^{a}
	20	**2550**	**22.4**	**26.1 ± 1.6^{a}**
	30	2470	25.5	27.1 ± 0.2^{a}
	40	2313	27.7	42.4 ± 2.7^{c}
PAN	5	4567	14.3	34.7 ± 3.7^{b}
	15	3823	15.8	37.5 ± 1.3^{bc}
	30	3421	16.9	31.2 ± 0.1^{b}
	60	**2897**	**23.7**	**32.3 ± 1.6^{b}**
	120	2634	25.8	39.7 ± 3.2^{c}
	240	2150	29.8	41.9 ± 0.9^{c}
TRY	30	15 341	5.2	25.9 ± 1.7^{a}
	60	12 321	8.5	28.9 ± 0.7^{a}
	120	5432	12.3	26.9 ± 2.5^{a}
	240	**5356**	**14.5**	**26.2 ± 0.1^{a}**
	480	3961	16.2	27.3 ± 0.3^{a}
	1440	2921	22.4	25.9 ± 1.6^{a}
PEG negative control				53.4 ± 0.8^{d}
PEG-ALC				56.2 ± 1.1^{de}
PEG-PAN				54.1 ± 1.1^{d}
PEG-TRY				58.3 ± 1.4^{e}
unhydrolyzed SPI		40 450		59.9 ± 2.3^{efive}

Values with different letters within the MLGS column are significantly different ($p < 0.05$). The bold samples were used to fractionate into five different MW ranges. Abbreviations: MW, molecular weight; DOH, degree of hydrolysis; ALC: Alcalase; PAN, pancreatin; TRY, trypsin.

Effect of the Extent of Hydrolysis on the IRI Activity of SPI Hydrolysates. Hydrolysis time, however, did not play a significant role in IRI activity. There were a few notable exceptions that a reduction in IRI activity was seen due to hydrolysis; SPI-ALC-40 (the number indicates the time of hydrolysis, in min), SPI-PAN-120, and SPI-PAN-240 had MLGSs of 42.4 ± 2.7, 39. 7 ± 3.2, and 41.9 ± 0.9 μm, respectively. This was a significant increase in MLGS when compared to all of the other hydrolysate samples, indicating a decrease in IRI activity. To demonstrate the effect of extensive hydrolysis on IRI activity, another hydrolysis using ALC was performed at the same concentration and hydrolysis conditions as used previously, but the time was extended to include 40, 45, and 50 min and a sample was also taken at 20 min to ensure the sample still had activity. The IRI activity of these hydrolysates was similar to the previous SPI-ALC-40 sample. All SPI-ALC-40, 45, and 50 samples showed a decrease in IRI activity when compared to the 20 min sample taken from the same test run. This highlights that a reduction of IRI activity from extensive protein hydrolysis is an issue if the hydrolysis reaction is not controlled properly.

Previously, it was reported for bovine gelatin and fish gelatin that the samples had an optimum hydrolysis time of 30 min to produce the best IRI active peptides of 600−2500 Da and 25 min to produce 800−3300 Da peptides, respectively.[27,28] These results are different from the SPI hydrolysates reported

https://doi.org/10.1021/acs.jafc.2c08701
J. Agric. Food Chem. XXXX, XXX, XXX−XXX

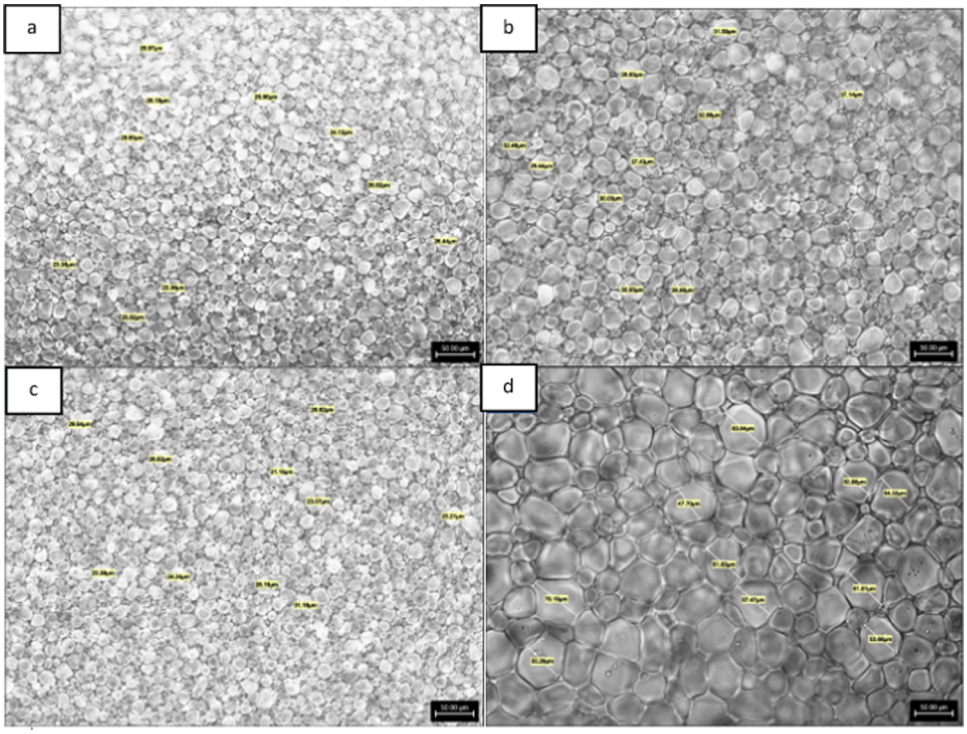

Figure 2. Representative microscopy images (scale bar = 50 μm) obtained by splat assay measurements at a 4% concentration of SPI hydrolyzed by ALC for 5 min (a), PAN for 30 min (b), TRY for 8 h (c), and 4% PEG negative control (d).

in this study. The difference could be due to the amino acid composition and sequence difference between soy protein and gelatin, in a manner that the activity mechanism for ice recrystallization could be different and this would lead to different optimal molecular characteristics. It is also possible due to the high concentration of proline and hydroxyproline that contribute to a more rigid secondary structure of peptides, so a shorter peptide chain may be needed than SPI peptides, which may need a longer chain to form a desirable secondary structure. This observation may point to the importance of peptide folding or intra- or intermolecular assembly being an important feature of IRI activity for this class of compounds.

However, the fact that prolonged hydrolysis decreased the IRI activity of the peptides was consistent between the previous studies and this work.[27,28] Even though there was no difference in IRI activity between the SPI hydrolysates produced from the same enzyme, with the exceptions noted previously, all of the SPI hydrolysates showed a significantly reduced MLGS when compared to unhydrolyzed SPI (59.9 ± 2.3 μm) and the PEG negative control (53.4 ± 0.8 μm), which indicates IRI activity for all of the whole SPI hydrolysate samples. Even though the average MWs of the samples are different, each sample is a mixture of peptides, so relationships between peptide size and IRI activity cannot be identified with these data. Therefore, further separation was necessary to understand how the MW of the hydrolysates affects IRI activity.

Fractionation of SPI Hydrolysates and the Effect of Peptide Size on IRI Activity. Selected SPI-derived peptides having IRI activity were fractionated into five different fractions (F1−F5) by preparative size exclusion chromatography. The IRI activity of each of these fractions was measured and is summarized in Table 2. An illustration of how the fractions were collected is shown in Figure 3. The most IRI active fraction for each sample was the first fraction (F1), which was the only fraction for all three samples that had similar IRI activity compared to the whole hydrolysate (SPI-ALC-20 = 29.3 ± 0.2 μm, SPI-ALC-20-F1 = 24.4 ± 1.1 μm; SPI-PAN-60 = 28.7 ± 1.2 μm, SPI-PAN-60-F1= 31.2 ± 4.8 μm; SPI-TRY-120 = 29.8 ± 0.5 μm, SPI-TRY-120-F1 = 29.3 ± 1.3 μm). The fractions (F2−F3) still maintained a slight IRI

Table 2. MLGS Tested at 4% Concentration, Mass %, and Average MW from Fractionated SPI Hydrolysates by Preparative Size Exclusion Chromatography

enzyme/sample	fraction	MLGS (μm)	mass, %	average MW (Da)
SPI-TRY-120	F1	29.3 ± 1.3^{b}	18.8	10 037.6
	F2	48.6 ± 3.4^{c}	13.3	3344.1
	F3	43.7 ± 0.7^{c}	36.3	498.2
	F4	70.7 ± 3.5^{e}	28.4	215
	F5	65.2 ± 1.6^{e}	3.2	156.1
	whole	29.8 ± 0.5^{b}	100	18 951.3
SPI-PAN-60	F1	32.2 ± 4.8^{b}	21.2	13 435.7
	F2	41.6 ± 2.0^{c}	15.6	1203.2
	F3	37.5 ± 2.8^{c}	22.9	372.4
	F4	69.1 ± 4.5^{e}	37.7	134.4
	F5	69.5 ± 2.2^{e}	2.6	214.6
	whole	28.7 ± 1.2^{b}	100	15 685.8
SPI-ALC-20	F1	24.4 ± 1.1^{a}	8.4	4903.9
	F2	42.8 ± 0.4^{c}	33.6	1456.6
	F3	41.6 ± 2.0^{c}	25.6	530.0
	F4	66.3 ± 1.3^{e}	30.9	305.7
	F5	62.1 ± 3.4^{e}	1.4	121.1
	whole	29.3 ± 0.2^{b}	100	1391.7
4% PEG		53.4 ± 0.8^{d}		

Values with different letters within the MLGS column are significantly different ($p < 0.05$). For all abbreviations, please refer to the footnote in Table 1.

https://doi.org/10.1021/acs.jafc.2c08701
J. Agric. Food Chem. XXXX, XXX, XXX−XXX

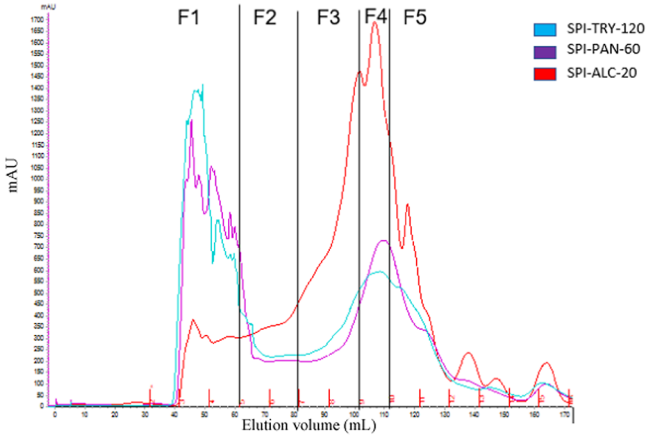

Figure 3. Representative fractionation chromatograph by preparative size exclusion chromatography of SPI-TRY-120 (blue), SPI-PAN-60 (purple), and SPI-ALC-20 (red).

activity when compared to the negative control PEG but were not as effective as the whole hydrolysate or the F1 fraction. F4 and F5 (with ice crystal size of >60 μm), which contained the smallest peptides (all with average MWs lower than 500 Da) for all hydrolysates, showed no IRI activity relative to the negative control (4% PEG = 53.4 ± 0.8 μm). All fractions are still mixtures of peptides with different MWs and proportions, as discussed in the following sections.

The data show that the F1 fraction had similar activity as the whole hydrolysate for all three samples (Table 2), even though F1 is only a small weight fraction of the whole. In this case, the mass action law or the "dilution effect" does not apply, since F1 and whole matrix compositions (peptide profile) are different (Figure 5). Nonetheless, how the molecules of different sizes and peptide sequences work together in such complex mixtures is unknown. These molecules may work together to form different types of molecular complexes to lead to different physicochemical properties,[44,45] and much is to be discovered.

Dilution of Whole and Fractionated SPI Samples to Compare IRI Strength at Lower Concentrations. The activity from the F1 fractions suggests that most of the IRI activity comes from the larger peptides regardless of enzyme specificity, and the large peptides need to be present for the strong activity. This would explain why the hydrolysates with the highest DOH had a reduction in IRI activity compared to the other samples. This could also mean that the IRI activity from the whole hydrolysate samples could be due to the large peptides contained in the F1 fraction, and these samples could be effective at lower concentrations than 4%. To test this, both the F1 fractions and the whole hydrolysate samples were diluted to 2 and 1% and the MLGS results from this dilution are detailed in Table 3. Depending on the protease used for hydrolysis, the F1 fractions behaved differently compared to the whole hydrolysate, and the most active sample was SPI-ALC-20-F1. This fraction had a smaller increase in MLGS compared to the other two samples when the concentration decreased from 4% (F1 = 24.4 ± 0.1 μm) to 2% (F1 = 28.5 ± 1.9 μm) and had significantly higher activity than the whole hydrolysate at 2% (49.1 ± 3.2 μm). This was not the same pattern for SPI-PAN-60 and SPI-TRY-120. SPI-PAN-60-F1 had higher activity than the whole hydrolysate at 2 and 1% concentrations and had similar IRI activity at 4%, but all activity was lower than that of Alcalase hydrolysate samples.

Table 3. IRI Activity (MLGS) of SPI Hydrolysates and Their F1 Fractions Tested at Varying Concentrations

		MLGS (μm)	
sample	concentration (%)	F1	whole
SPI-TRY-120	4	32.4 ± 2.0^{a}	29.8 ± 0.5^{a}
	2	63.1 ± 5.52^{b}	58.6 ± 0.9^{b}
	1	88.4 ± 1.8^{c}	87.5 ± 5.7^{c}
SPI-PAN-60	4	31.2 ± 3.2^{a}	28.7 ± 1.2^{a}
	2	46.6 ± 0.3^{b}	67.5 ± 9.4^{d}
	1	52.1 ± 7.1^{c}	72.7 ± 6.1^{e}
SPI-ALC-20	4	24.4 ± 0.1^{a}	29.3 ± 0.2^{b}
	2	28.5 ± 1.9^{b}	49.1 ± 3.2^{c}
	1	51.4 ± 5.6^{cd}	54.9 ± 0.6^{d}

Values with different letters for F1 and the whole fraction for each sample are significantly different ($p < 0.05$). For all abbreviations, please refer to the footnote in Table 1.

The SPI-TRY-120-F1 sample maintained similar IRI activity as the whole hydrolysate regardless of the concentration.

It is clearly shown that different molecular size fractions (F1−F5) from the SPI hydrolysate had different IRI activities and that the same fractions also had different IRI activities when varying concentrations (1−4%). SPI-PAN-60-F1 fraction and SPI-TRY-120-F1 samples seem to have a similar MW distribution (Figure 5), but the concentration of the sample affected the IRI activity differently. At a higher concentration, the trypsin hydrolyzed samples had a higher activity than pancreatin samples at 4% (Tables 1−3), but after dilution to 2%, the pancreatin samples maintained lower ice crystal size. The SPI-ALC-20-F1 sample, however, maintained the strongest activity at 4 and 2% when compared to all samples.

These differences could be due to the peptide composition difference in hydrolysates among the samples, and the largest peptides in SPI-TRY and SPI-PAN samples are too large for strong activity. For instance, TRY and PAN being amino acid specific enzymes would cleave less than ALC, resulting in peptides with higher MWs and different molecular characteristics. In gelatin peptides, it is hypothesized that peptides over the size of 6.5 kDa cannot readily change their conformation and therefore had high steric hindrance, which contributes to the large peptides lacking IRI activity.[16] However, gelatin/collagen protein and peptides have a more rigid coil/helical structure, whereas soy peptides are produced from albumin and globulin proteins,[43] which naturally have more flexibility. This aspect could lead to differences in the flexibility of peptides derived from different sources and therefore differing functional sizes, with the larger soy peptides having more flexibility than the larger gelatin peptides. However, there must be a size that is too large for activity because the soy protein itself lacks activity. In Figure 5, the MW ratios of less than 1 kDa, 1−5 kDa, and greater than 5 kDa all seemed similar when the amounts of F1 fractions are compared, but when observing the elution profiles, the SPI-PAN-60-F1 and SPI-TRY-120-F1 samples had peptides leaving the column at shorter retention times compared to the Alcalase sample, indicating that while they have a similar amount of peptides above 5 kDa, their peptides are much larger than that in the Alcalase sample. This indicates that the MW of the larger peptides or MW distribution profile of the sample is very important for a stronger IRI activity and should be studied more in depth. This can explain why after fractionation, SPI-TRY-120-F1 had similar IRI activity to the whole hydrolysate and was weak

https://doi.org/10.1021/acs.jafc.2c08701
J. Agric. Food Chem. XXXX, XXX, XXX−XXX

compared to SPI-ALC-20-F1. SPI-TRY-120 had the highest amount of high-MW peptides and the lowest amount of low-MW peptides compared to both SPI-ALC-20 and SPI-PAN-60. It can be seen in Table 3 that the IRI activity of SPI-TRY-120-F1 and whole SPI-TRY-120 remained very similar at all concentrations, and the IRI activity is lost very fast with concentration reduction. SPI-ALC-20 contained the highest amount of low-MW peptides and the lowest amount of high-MW peptides, and after fractionation, the F1 fraction had a relatively higher IRI activity even at 2 and 1% concentrations than whole hydrolysates. The F1 fraction at 2% (28.5 ± 1.9 μm) maintained the same activity as the 4% SPI-ALC-20 (24.4 ± 0.1 μm) and was the strongest sample tested. This means that a more ideal mixture for the maximum IRI activity could have been produced with a reduction of low-MW peptides in SPI-ALC-20.

It should be stressed that the effective size of the large peptides has to be better defined. Accurate molecular weight and profile determination are crucial in this effort, and average molecular weight does not provide enough information. Even though the MW% presented in the bar graph in Figure 5 can be similar, the size of the peptides in the large molecular weight range can be different, as the MW of the large peptides in the SPI-TRY-120 sample is much larger than that in the SPI-ALC-20 sample. Another important factor in evaluating the IRI activity of different matrices is the concentration of the peptides used as demonstrated in this study.

MW of the Whole and Fractionated Peptides by SDS-PAGE, HPLC, and LC-MALDI-TOF. To determine the size of the peptides in the various fractions, MW distributions of F1−F5 fractions for SPI-ALC-20, SPI-PAN-60, and SPI-TRY-120 were measured by both SDS-PAGE and HPLC and are presented in Figures 4 and 5. In Figure 4, notably, the F1

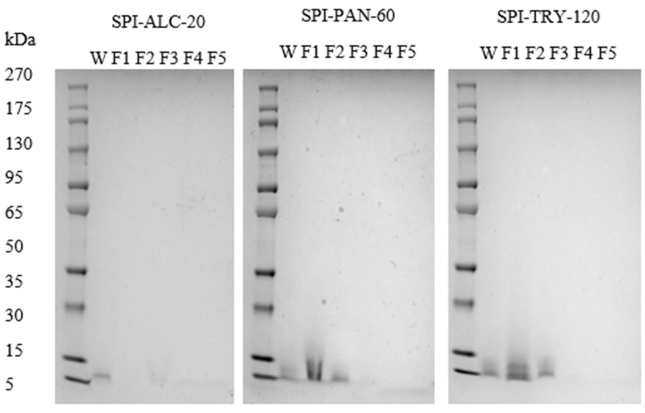

Figure 4. SDS-PAGE gels of starting whole SPI samples of SPI-ALC-20, SPI-PAN-60, and SPI-TRY-120, and fractions 1−5 collected from preparative size exclusion chromatography. W stands for the whole hydrolysate.

fraction of SPI-TRY-120 in lane 3 of the SDS-PAGE gels had the most noticeable bands between the 5 and 15 kDa markers. The F2 fraction for SPI-TRY-120 and SPI-PAN-60 also contained some protein staining between 5 and 15 kDa, but most color was toward the 5 kDa marker, indicating that the peptides were closer to 5 kDa than 15 kDa. The F2 fraction for all samples showed a reduction in IRI activity when compared to the F1 fraction, as shown in Table 2. This means that the peptides closer to 15 kDa could be responsible for the majority of the IRI activity of the SPI-PAN and SPI-TRY hydrolysates or at least are required for a stronger IRI activity. Given that Coomassie blue is not as reactive to smaller peptides and amino acids,[46] the absence of these bands in samples F3−F5 regardless of protease used supports the fact that there is a lack of IRI active peptides in these samples. This is supported further by HPLC data in Figure 5 and Table 2, which show that these fractions contain smaller peptides with a calculated average MW of 530 Da or less that are not effectively stained by Coomassie blue in SDS-PAGE analysis.

The HPLC and SDS-PAGE data show a separation of the larger peptides in F1 and F2 samples, which was expected. However, as shown in Figure 5, smaller peptides can also be seen in the F1 and F2 fractions, meaning it was not a clean separation and that the F1 and F2 fractions still contain a mixture of peptides. However, since they are the only fractions with strong IRI activity, it suggests that the large peptides are the most important peptides for activity. The average MWs for F1 for both SPI-TRY-120 and SPI-PAN-60 are slightly smaller than the whole hydrolysate, which was not expected but can be explained. The F1 fractions, in theory, should have a larger average MW due to fewer lower MW peptides in the samples and therefore a greater percentage of larger peptides. The F1 fractions having a lower average MW could arise, since all samples were centrifuged and filtered before fractionation to remove insoluble molecules (if present within the ammonium bicarbonate buffer used for fractionation), whereas the whole fractions only underwent one centrifugation after hydrolysis. Both PAN and TRY samples had a small portion of particulates formed when added to the ammonium bicarbonate buffer instead of water, which was removed before filtering and HPLC separation. This could correspond to the lower MW of the F1 fraction. Based on the HPLC data in Table 2, all F3−F5 samples had an average MW lower than 530 Da, indicating that peptides consisting of 1−4 amino acids are too small to generate appreciable IRI activity in the 1× PBS buffer used for testing. The SPI-ALC-20-F1 sample did not appear on SDS-PAGE and had a weak intensity when measured by HPLC in Figure 5a. This can be due to the sample not being concentrated enough for an accurate analysis, or the smaller peptides not being effectively stained.

To further support this claim, F1 and F4 fractions were analyzed using LC-MS (MALDI-TOF) to measure molecular size. The molecular species profiles (shown in Figure 6) of the F1 and F4 fractions were consistent with HPLC and SDS-PAGE data where the F1 fractions contained larger peptides that the F4 fraction lacked, and the F1 fraction is a mixture of low- and high-MW peptides. However, the size of the larger peptides could not be confirmed because this method only accurately measured between 6 and 30 amino acid residues.

We note that F1 being the most IRI active fraction was not expected, as it was hypothesized that the active peptides would be between the sizes of 1 and 5 kDa as reported by others.[16−30] In the case of fish gelatin, it was even stated that all peptides above the MW of 6500 Da did not show IRI activity.[27,28] This means that the larger SPI peptides are more effective in IRI applications, whereas smaller peptides were more effective for bovine,[16] fish,[17] and shark[28,29] gelatins. This suggests that the larger peptides in the SPI hydrolysates possessed certain amino acid sequences and structural properties that lead to their IRI activity, and the gelatin peptides of similar sizes did not. Amino acid composition is another important factor, but its effect is very difficult to be generalized. These results further emphasize

https://doi.org/10.1021/acs.jafc.2c08701
J. Agric. Food Chem. XXXX, XXX, XXX−XXX

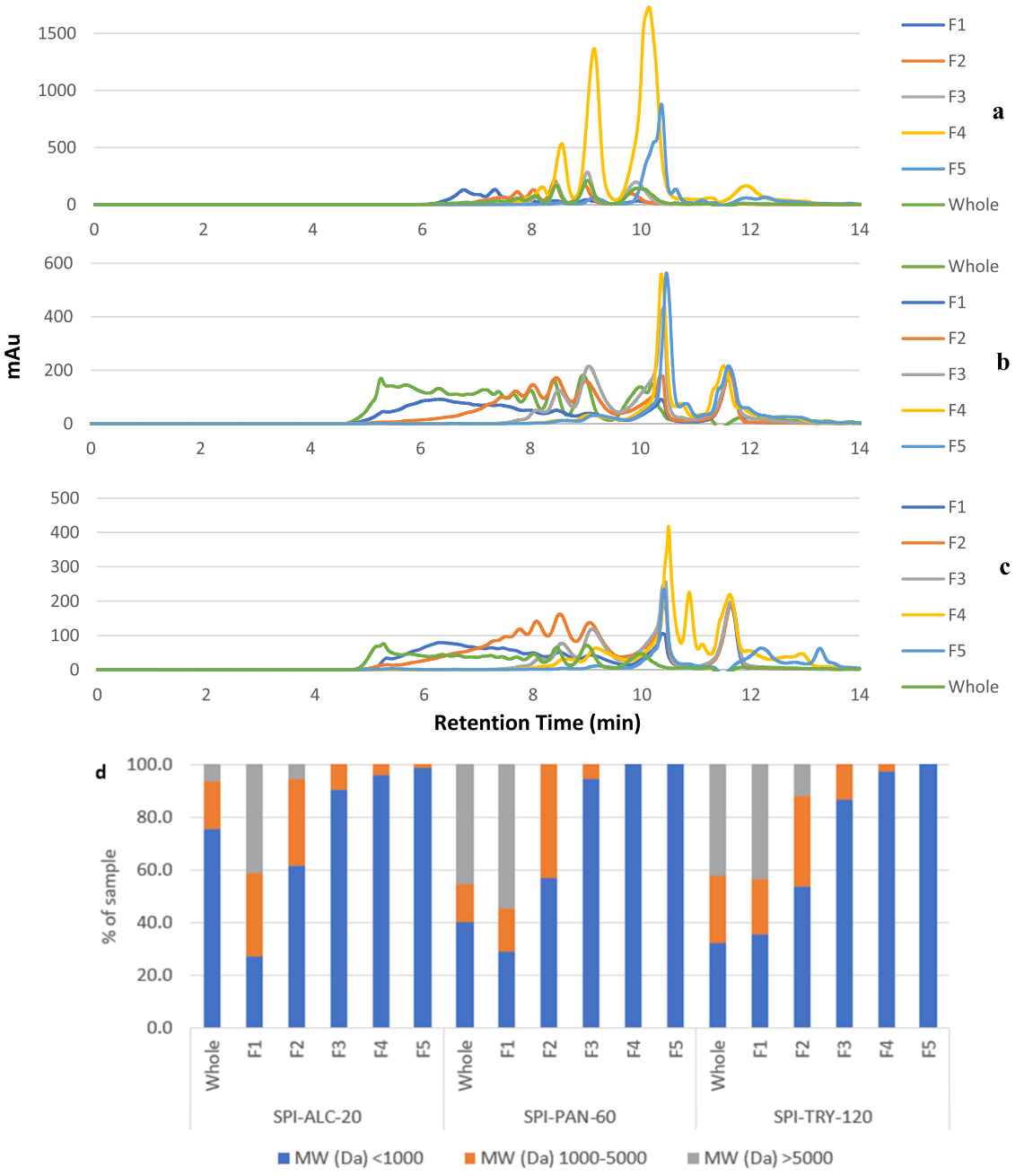

Figure 5. HPLC elution profile of fractions 1−5 for SPI-ALC-20 (a), SPI-PAN-60 (b), and SPI-TRY-120 (c) compared to the whole hydrolysate, and the MW profiles quantified by HPLC (d).

the fact that the mechanism underlying IRI activity in SPI-derived compounds and from other proteins could be different, presumably due to differences in the amino acid composition, sequences, or secondary structures of the peptides. It also can be concluded that the protease used can affect IRI activity due to the difference in size and secondary structure of peptides.

Surface Partitioning of Peptides and F1 Fractions. To understand the interfacial behavior of the peptides and how their molecular characteristics and interactions relate to the IRI activity, SPI-derived peptides were probed at the air−aqueous interface by vibrational sum frequency generation (VSFG) measurements. The VSFG intensity can be used to understand both how peptide molecules assemble at the air−aqueous interface and provide insights into their relative concentrations.

Figure 7 shows spectra from SPI hydrolysates and their F1 fractions compared with the spectra obtained from the unhydrolyzed SPI. In the CH stretching region (~2800 to 3000 cm^{-1}), we find that the F1 and whole hydrolysate mixtures from SPI-PAN-60 and SPI-TRY-120 hydrolysate samples generated similar spectra compared to each other and the whole SPI protein with only subtle differences in peak intensities. This suggests that the major surface-active component is contained in F1, in agreement with similar IRI activities. However, we find that the VSFG response in the CH stretching region from SPI-ALC-20-F1 is notably larger than that of the SPI-ALC-20 whole hydrolysate. The higher intensity observed for SPI-ALC-20-F1 indicates that amphiphilic species are strongly partitioned to the air−aqueous

https://doi.org/10.1021/acs.jafc.2c08701
J. Agric. Food Chem. XXXX, XXX, XXX−XXX

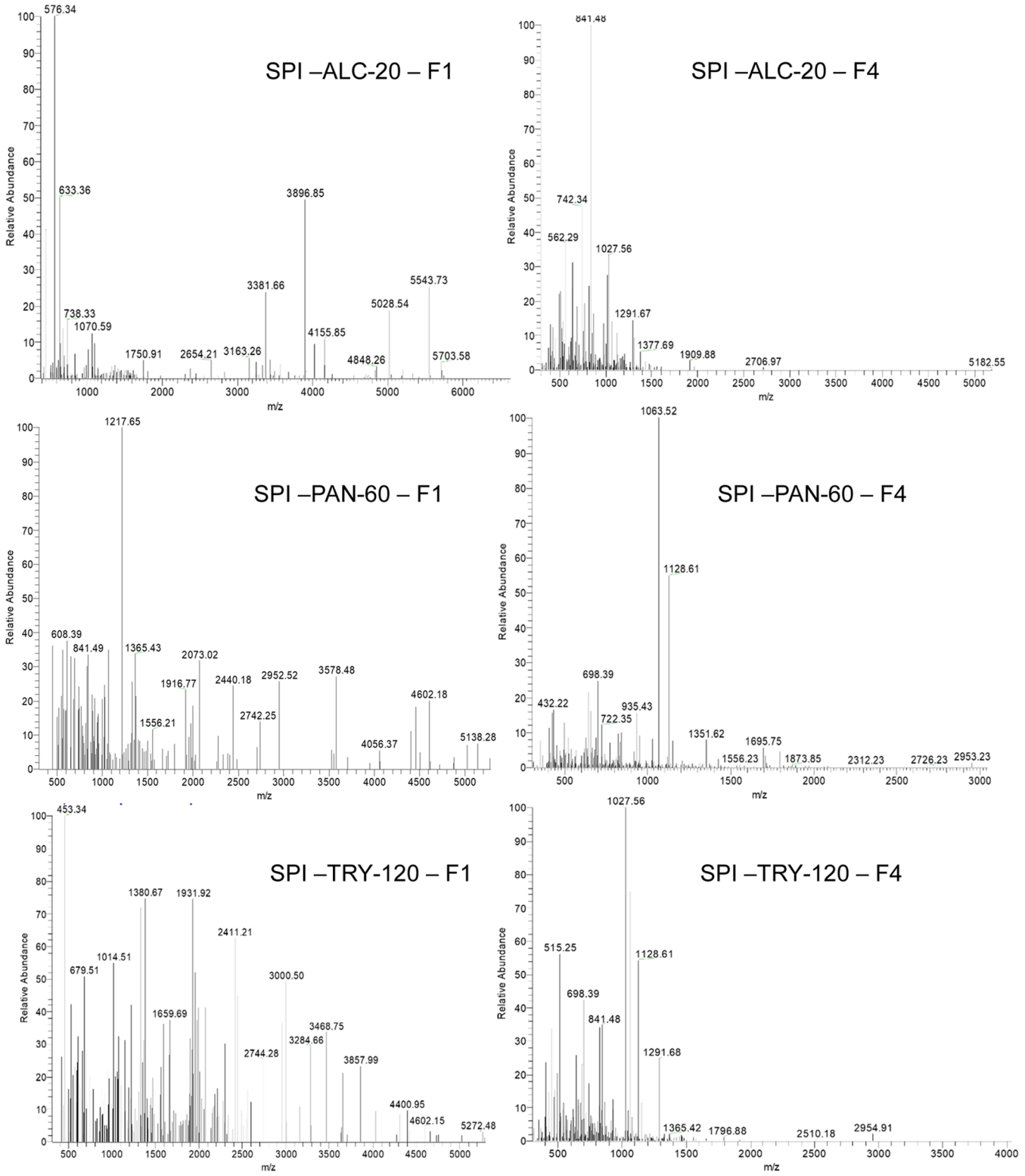

Figure 6. Mass spectra for SPI-ALC-20, SPI-PAN-60, and SPI-TRY-120′s F1 and F4 fractions measured by LC-MALDI-TOF.

interface and that their hydrophobic groups are well-ordered compared to the other peptides. This could be due to better packing, stronger hydrophobic-driven alignment, or higher surface densities. This holds true for control samples as well, where the positive control (PVA) has more intense and better resolved peaks suggestive of a better ordered interfacial layer than the negative control (PEG), which has weak and spectrally broad features. Incidentally, molecular self-assembly and hydrophobicity-driven alignment have been hypothesized to be a mechanism of IRI activity in the literature. When compared to IRI activities, spectra from all hydrolyzed peptides except whole SPI-ALC-20 are of higher intensities than that of the unhydrolyzed SPI. The similar VSFG spectral responses of whole SPI-ALC-20 and unhydrolyzed SPI with disparate IRI

https://doi.org/10.1021/acs.jafc.2c08701
J. Agric. Food Chem. XXXX, XXX, XXX−XXX

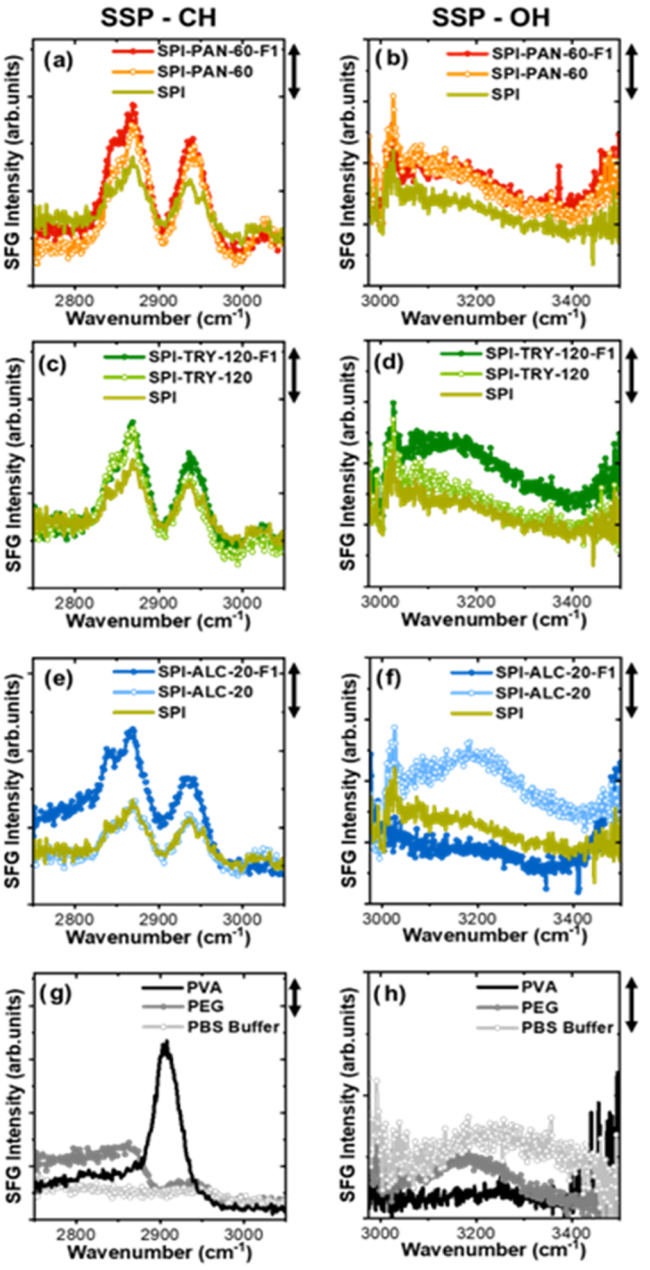

Figure 7. Vibrational sum frequency generation spectra acquired at CH and OH vibrational regions from SPI-PAN-60 (a, b), SPI-TRY-120 (c, d), SPI-ALC-20 (e, f), and their F1 fractions compared with unhydrolyzed SPI in 1× PBS buffer. PEG and 1× PBS buffer spectra are shown in (g, h). The scale bar represents 0.25 au.

activities suggest that in the case of unhydrolyzed SPI, surface sites are largely occupied with species that give poorer IRI properties.

To further understand how the interface changes with these peptides of varying IRI activities, we acquired SFG spectra from the OH stretching region. This vibrational region (from ~3100 to ~3500 cm^{-1}) reports on the hydrogen bonding network at the interface and the degree of surface charging arising from ionized residues.[47,48] As shown in Figure 7b, we find that the H-bonding signals are generally shifted to lower frequencies compared to the whole SPI sample, indicating that PAN hydrolysates force water to assume a more strongly bound interfacial H-bond network. Given the experiments were performed in 1x PBS buffer, effects from the surface potential from the charged peptides are assumed to be screened. Similar effects are seen for SPI-TRY-120 and its F1 fraction (Figure 7d), indicating stronger H-bonding and better ordering of water in the presence of the F1 sample and suggestive of a relationship between water ordering and IRI activity. On the other hand, both whole SPI and SPI-ALC-20 show stronger OH signals than the SPI-ALC-20-F1 sample, as plotted in Figure 7f. Notably, the SPI-ALC-20-F1 sample weakly orders water but has enhanced ordering of hydrophobic groups (evidenced by the CH stretches). These observations point to a complex relationship between hydrophobicity and H-bonding interactions that compete in IRI activity relationships. These relationships can vary from sample to sample, for example, in PEG, the OH spectra are suggestive of stronger H-bonding interactions with the polymer, but the IRI response from the polymer itself is weak. Considering that PVA is the strongest IRI agent, it was expected that the H-bonding would be the strongest. The weak H-bonding signal from the PVA positive control and strong hydrophobic ordering could indicate that the ordering of the hydrophobic groups is more important to IRI activity. This could explain why the strongest IRI sample (SPI-ALC-20-F1) had the lowest H-bonding intensity out of all of the SPI samples tested. Continued work is needed and underway to understand the competition between the amphiphilicity of the peptides, associated interactions with water, and how to control the interplay between these interactions at interfaces to enhance IRI activities. We emphasize here that SFG measurements probing the peptides at the air/water interface do not inform on the structures or assemblies that would form at the ice/water interface. However, based on the current understanding of IRI, the amphiphilicity of the peptide is a key factor governing ice crystal growth. The SFG measurements here are demonstrative that the amphiphilicity of the peptide changes (e.g., differences in the SFG response at the air/water interface) based on hydrolysis conditions and that these results parallel IRI activities measured above.

In summary, we have demonstrated that soy protein hydrolysates have IRI activity. All SPI samples hydrolyzed by ALC, TRY, and PAN produced IRI active peptides, but the TRY and ALC hydrolysates had higher activity compared to PAN hydrolyzed peptides. The hydrolysis time was not significant when compared among the active hydrolysates, but the hydrolysates did have a reduction in IRI activity due to extensive hydrolysis for PAN and ALC. After size fractionation, the larger peptides in the F1 fraction were shown to have the highest IRI activity compared to all other fractions, but they were still a mixture of large and small peptides. Regardless, there seems to be a need for larger MW peptides within the sample to have strong activity, and the effective size needs to be better defined. VSFG measurements showed differences in the surface activities of various peptides and their influence on water structuring. These experiments support observations made on IRI activity. This work is anticipated to provide more insights into the development and refinement of plant protein-based IRI agents and new evaluation methods to identify the key features for IRI activity in a mixture of peptides.

AUTHOR INFORMATION

Corresponding Author

Tong Wang − *Department of Food Science, The University of Tennessee, Knoxville, Tennessee 37994, United States;*

https://doi.org/10.1021/acs.jafc.2c08701
J. Agric. Food Chem. XXXX, XXX, XXX−XXX

orcid.org/0000-0002-6667-6498; Phone: 865-974-7279; Email: twang46@utk.edu

Authors

Madison Fomich − *Department of Food Science, The University of Tennessee, Knoxville, Tennessee 37994, United States*

Vermont P. Día − *Department of Food Science, The University of Tennessee, Knoxville, Tennessee 37994, United States;* orcid.org/0000-0003-2804-4323

Uvinduni I. Premadasa − *Chemical Sciences Division, Oak Ridge National Laboratory, Oak Ridge, Tennessee 37831, United States;* orcid.org/0000-0003-0289-2965

Benjamin Doughty − *Chemical Sciences Division, Oak Ridge National Laboratory, Oak Ridge, Tennessee 37831, United States;* orcid.org/0000-0001-6429-9329

Hari B. Krishnan − *Plant Genetics Research Unit, Agricultural Research Service, USDA, Columbia, Missouri 65211, United States*

Complete contact information is available at: https://pubs.acs.org/10.1021/acs.jafc.2c08701

Notes

The authors declare no competing financial interest.

This manuscript has been co-authored by UT-Battelle, LLC, under contract DE-AC05-00OR22725 with the US Department of Energy (DOE). The US government retains and the publisher, by accepting the article for publication, acknowledges that the US government retains a nonexclusive, paid-up, irrevocable, worldwide license to publish or reproduce the published form of this manuscript or allow others to do so, for US government purposes. DOE will provide public access to these results of federally sponsored research in accordance with the DOE Public Access Plan (http://energy.gov/downloads/doe-public-access-plan).

■ ACKNOWLEDGMENTS

This work is supported by an NSF grant [Award Number: 2103558] and Hatch/Multi-state project [Accession Number: 1023982].

■ ABBREVIATIONS

SPI, soy protein isolate; IRI, ice recrystallization inhibition; VSFG, vibrational sum frequency generation; MW, molecular weight; prep-MPLC, preparative medium pressure chromatography; ALC, Alcalase; TRY, trypsin; PAN, pancreatin; HPLC, high-performance liquid chromatography; F1−F5, fractions 1−5; AFPs, antifreeze proteins; AFGPs, antifreeze glycoproteins; PVA, poly(vinyl alcohol); PEG, poly(ethylene glycol); IR, infrared; NIR, near infrared; MLGS, mean largest grain size; Da, dalton; kDa, kilodalton; DOH, degree of hydrolysis

■ REFERENCES

(1) Capicciotti, C. J.; Doshi, M.; N, R. Ice Recrystallization Inhibitors: From Biological Antifreezes to Small Molecules. In *Recent Developments in the Study of Recrystallization*; Wilson, P., Ed.; InTech, 2013.

(2) Knight, C. A.; Wen, D.; Laursen, R. A. Nonequilibrium Antifreeze Peptides and the Recrystallization of Ice. *Cryobiology* **1995**, *32*, 23−34.

(3) Li, D.; Zhu, Z.; Sun, D.-W. Effects of Freezing on Cell Structure of Fresh Cellular Food Materials: A Review. *Trends Food Sci. Technol.* **2018**, *75*, 46−55.

(4) Buckley, S. L.; Lillford, P. J. Antifreeze Proteins. In *Modern Biopolymer Science*; Elsevier, 2009; pp 93−128.

(5) Graham, L. A.; Davies, P. L. Glycine-Rich Antifreeze Proteins from Snow Fleas. *Science* **2005**, *310*, 461.

(6) Graham, L. A.; Liou, Y.-C.; Walker, V. K.; Davies, P. L. Hyperactive Antifreeze Protein from Beetles. *Nature* **1997**, *388*, 727−728.

(7) Graether, S. P.; Sykes, B. D. Cold Survival in Freeze-Intolerant Insects: The Structure and Function of β-Helical Antifreeze Proteins. *Eur. J. Biochem.* **2004**, *271*, 3285−3296.

(8) Jia, Z.; Davies, P. L. Antifreeze Proteins: An Unusual Receptor−Ligand Interaction. *Trends Biochem. Sci.* **2002**, *27*, 101−106.

(9) Griffith, M.; Ewart, K. V. Antifreeze Proteins and Their Potential Use in Frozen Foods. *Biotechnol. Adv.* **1995**, *13*, 375−402.

(10) Kontogiorgos, V.; Regand, A.; Yada, R. Y.; Goff, H. D. Isolation andCharacterization of Ice Structuring Proteins from Cold-acclimated Winter Wheat Grass Extract for Recrystallization Inhibition inFrozenFoods. *J. Food Biochem.* **2007**, *31*, 139−160.

(11) Kristiansen, E.; Ramløv, H.; Hagen, L.; Pedersen, S. A.; Andersen, R. A.; Zachariassen, K. E. Isolation and Characterization of Hemolymph Antifreeze Proteins from Larvae of the Longhorn Beetle Rhagium Inquisitor (L.). *Comp. Biochem. Physiol., Part B: Biochem. Mol. Biol.* **2005**, *142*, 90−97.

(12) Li, L.; Wu, J.-H.; Zhang, L.; Chen, X.; Wu, Y.; Liu, J.; Geng, X.; Wang, Z.-W.; Wang, S.-Y. Investigation of the Physicochemical Properties, Cryoprotective Activity and Possible Action Mechanisms of Sericin Peptides Derived from Membrane Separation. *LWT − Food Sci. Technol.* **2017**, *77*, 532−541.

(13) Pentelute, B. L.; Gates, Z. P.; Dashnau, J. L.; Vanderkooi, J. M.; Kent, S. B. H. Mirror Image Forms of Snow Flea Antifreeze Protein Prepared by Total Chemical Synthesis Have Identical Antifreeze Activities. *J. Am. Chem. Soc.* **2008**, *130*, 9702−9707.

(14) Worrall, D.; Elias, L.; Ashford, D.; Smallwood, M.; Sidebottom, C.; Lillford, P.; Telford, J.; Holt, C.; Bowles, D. A Carrot Leucine-Rich-Repeat Protein That Inhibits Ice Recrystallization. *Science* **1998**, *282*, 115−117.

(15) Chen, X.; Wu, J.; Cai, X.; Wang, S. Production, Structure−Function Relationships, Mechanisms, and Applications of Antifreeze Peptides. *Compr. Rev. Food Sci. Food Saf.* **2021**, *20*, 542−562.

(16) Damodaran, S. Inhibition of Ice Crystal Growth in Ice Cream Mix by Gelatin Hydrolysate. *J. Agric. Food Chem.* **2007**, *55*, 10918−10923.

(17) Damodaran, S.; Wang, S. Ice Crystal Growth Inhibition by Peptides from Fish Gelatin Hydrolysate. *Food Hydrocolloids* **2017**, *70*, 46−56.

(18) Liou, Y.-C.; Tocilj, A.; Davies, P. L.; Jia, Z. Mimicry of Ice Structure by Surface Hydroxyls and Water of a β-Helix Antifreeze Protein. *Nature* **2000**, *406*, 322−324.

(19) Adapa, S.; Schmidt, K. A.; Jeon, I. J.; Herald, T. J.; Flores, R. A. Mechanisms Ice Crystallization and Recrystallization in Ice Cream: A Review. *Food Rev. Int.* **2000**, *16*, 259−271.

(20) Chen, X.; Wu, J.; Li, L.; Wang, S. The Cryoprotective Effects of Antifreeze Peptides from Pigskin Collagen on Texture Properties and Water Mobility of Frozen Dough Subjected to Freeze−Thaw Cycles. *Eur. Food Res. Technol.* **2017**, *243*, 1149−1156.

(21) Chen, X.; Wu, J.; Li, L.; Wang, S. Cryoprotective Activity and Action Mechanism of Antifreeze Peptides Obtained from Tilapia Scales on *Streptococcus Thermophilus* during Cold Stress. *J. Agric. Food Chem.* **2019**, *67*, 1918−1926.

(22) Cao, H.; Zhao, Y.; Zhu, Y. B.; Xu, F.; Yu, J. S.; Yuan, M. Antifreeze and Cryoprotective Activities of Ice-Binding Collagen Peptides from Pig Skin. *Food Chem.* **2016**, *194*, 1245−1253.

(23) Nguyen, C. T.; Yuan, M.; Yu, J. S.; Ye, T.; Cao, H.; Xu, F. Isolation of Ice Structuring Collagen Peptide by Ice Affinity Adsorption, Its Ice-Binding Mechanism and Breadmaking Performance in Frozen Dough. *J. Food Biochem.* **2018**, *42*, No. e12506.

(24) Lu, J.; Wang, Y.; Chen, B.; Xie, Y.; Nie, W.; Zhou, H.; Xu, B. Effect of Pigskin Gelatin Hydrolysate on the Porcine Meat Quality during Freezing. *Meat Sci.* **2022**, *192*, No. 108907.

(25) Yu, W.; Xu, D.; Zhang, H.; Guo, L.; Hong, T.; Zhang, W.; Jin, Y.; Xu, X. Effect of Pigskin Gelatin on Baking, Structural and Thermal Properties of Frozen Dough: Comprehensive Studies on Alteration of Gluten Network. *Food Hydrocolloids* **2020**, *102*, No. 105591.
(26) Du, L.; Betti, M. Chicken Collagen Hydrolysate Cryoprotection of Natural Actomyosin: Mechanism Studies during Freeze-Thaw Cycles and Simulated Digestion. *Food Chem.* **2016**, *211*, 791−802.
(27) Wang, S.; Damodaran, S. Ice-Structuring Peptides Derived from Bovine Collagen. *J. Agric. Food Chem.* **2009**, *57*, 5501−5509.
(28) Wang, S.; Agyare, K.; Damodaran, S. Optimisation of Hydrolysis Conditions and Fractionation of Peptide Cryoprotectants from Gelatin Hydrolysate. *Food Chem.* **2009**, *115*, 620−630.
(29) Limpisophon, K.; Iguchi, H.; Tanaka, M.; Suzuki, T.; Okazaki, E.; Saito, T.; Takahashi, K.; Osako, K. Cryoprotective Effect of Gelatin Hydrolysate from Shark Skin on Denaturation of Frozen Surimi Compared with That from Bovine Skin. *Fish Sci.* **2015**, *81*, 383−392.
(30) Wang, S.; Zhao, J.; Chen, L.; Zhou, Y.; Wu, J. Preparation, Isolation and Hypothermia Protection Activity of Antifreeze Peptides from Shark Skin Collagen. *LWT − Food Sci. Technol.* **2014**, *55*, 210−217.
(31) Wan, Z.; Fei, T.; Wang, T.; Wan, Z.; Fei, T.; Wang, T. Inhibition of Ice Crystal Growth by Protein Hydrolysates from Different Plant- and Animal-Based Proteins. *Food Mater. Res.* **2022**, *2*, 17.
(32) Spellman, D.; McEvoy, E.; O'Cuinn, G.; FitzGerald, R. J. Proteinase and Exopeptidase Hydrolysis of Whey Protein: Comparison of the TNBS, OPA and pH Stat Methods for Quantification of Degree of Hydrolysis. *Int. Dairy J.* **2003**, *13*, 447−453.
(33) Knight, C. A.; Hallett, J.; DeVries, A. L. Solute Effects on Ice Recrystallization: An Assessment Technique. *Cryobiology* **1988**, *25*, 55−60.
(34) Chowdhury, A. U.; Lin, L.; Doughty, B. Hydrogen-Bond-Driven Chemical Separations: Elucidating the Interfacial Steps of Self-Assembly in Solvent Extraction. *ACS Appl. Mater. Interfaces* **2020**, *12*, 32119−32130.
(35) Chowdhury, A. U.; Liu, F.; Watson, B. R.; Ashkar, R.; Katsaras, J.; Patrick Collier, C.; Lutterman, D. A.; Ma, Y.-Z.; Calhoun, T. R.; Doughty, B. Flexible Approach to Vibrational Sum-Frequency Generation Using Shaped near-Infrared Light. *Opt. Lett.* **2018**, *43*, 2038.
(36) Chowdhury, A. U.; Watson, B. R.; Ma, Y.-Z.; Sacci, R. L.; Lutterman, D. A.; Calhoun, T. R.; Doughty, B. A New Approach to Vibrational Sum Frequency Generation Spectroscopy Using near Infrared Pulse Shaping. *Rev. Sci. Instrum.* **2019**, *90*, No. 033106.
(37) Biggs, C. I.; et al. Mimicking the Ice Recrystallization Activity of Biological Antifreezes. When is a New Polymer "Active"? *Macromol. Biosci.* **2019**, *19*, No. 1900082.
(38) Doucet, D.; Otter, D. E.; Gauthier, S. F.; Foegeding, E. A. Enzyme-Induced Gelation of Extensively Hydrolyzed Whey Proteins by Alcalase: Peptide Identification and Determination of Enzyme Specificity. *J. Agric. Food Chem.* **2003**, *51*, 6300−6308.
(39) Graycar, T. P.; Bott, R. R.; Power, S. D.; Estell, D. A. Subtilisins. In *Handbook of Proteolytic Enzymes*; Elsevier, 2013; pp 3148−3155.
(40) de Castro, R. J. S.; Bagagli, M. P.; Sato, H. H. Improving the Functional Properties of Milk Proteins: Focus on the Specificities of Proteolytic Enzymes. *Curr. Opin. Food Sci.* **2015**, *1*, 64−69.
(41) Weinstein, M. J.; Doolittle, R. F. Differential Specificities of Thrombin, Plasmin and Trypsin with Regard to Synthetic and Natural Substrates and Inhibitors. *Biochim. Biophys. Acta* **1972**, *258*, 577−590.
(42) Appel, W. Chymotrypsin: Molecular and Catalytic Properties. *Clin. Biochem.* **1986**, *19*, 317−322.
(43) Denavi, G. A.; Pérez-Mateos, M.; Añón, M. C.; Montero, P.; Mauri, A. N.; Gómez-Guillén, M. C. Structural and Functional Properties of Soy Protein Isolate and Cod Gelatin Blend Films. *Food Hydrocolloids* **2009**, *23*, 2094−2101.
(44) Makam, P.; Gazit, E. Minimalistic Peptide Supramolecular Co-Assembly: Expanding the Conformational Space for Nanotechnology. *Chem. Soc. Rev.* **2018**, *47*, 3406−3420.
(45) Kim, B. J.; Yang, D.; Xu, B. Emerging Applications of Supramolecular Peptide Assemblies. *Trends Chem.* **2020**, *2*, 71−83.
(46) Berges, J. A.; Fisher, A. E.; Harrison, P. J. A Comparison of Lowry, Bradford and Smith Protein Assays Using Different Protein Standards and Protein Isolated from the Marine Diatom Thalassiosira Pseudonana. *Mar. Biol.* **1993**, *115*, 187−193.
(47) Lukas, M.; Schwidetzky, R.; Kunert, A. T.; Backus, E. H. G.; Pöschl, U.; Fröhlich-Nowoisky, J.; Bonn, M.; Meister, K. Interfacial Water Ordering Is Insufficient to Explain Ice-Nucleating Protein Activity. *J. Phys. Chem. Lett.* **2021**, *12*, 218−223.
(48) Roeters, S. J.; Golbek, T. W.; Bregnhøj, M.; Drace, T.; Alamdari, S.; Roseboom, W.; Kramer, G.; Šantl-Temkiv, T.; Finster, K.; Pfaendtner, J.; Woutersen, S.; Boesen, T.; Weidner, T. Ice-Nucleating Proteins Are Activated by Low Temperatures to Control the Structure of Interfacial Water. *Nat. Commun.* **2021**, *12*, No. 1183.

https://doi.org/10.1021/acs.jafc.2c08701
J. Agric. Food Chem. XXXX, XXX, XXX−XXX